AN AIRBORNE DOPPLER LIDAR

Charles A. DiMarzio
Raytheon Company

James W. Bilbro
Marshall Space Flight Center

ABSTRACT

A Pulsed CO_2 Doppler Lidar has been developed for airborne measurements of atmospheric wind fields. This device has been successfully utilized in the detection and measurement of mountain-wave turbulence and wind shear, and in the generation of time histories of wind-field variations in smooth flight. This Lidar is now in the process of being configured for measurement of the atmospheric flow fields surrounding severe convective storms.

This paper will provide a brief description of the system, a discussion of the Lidar System's Capabilities, a brief look at typical data provided by the system, and an overview of near-term program plans.

INTRODUCTION

The coherent pulsed Doppler Lidar, shown in figure 1, was built by the Raytheon Co. for NASA Marshall Space Flight Center in 1971 (ref. 1). This unit was originally designed for the detection of clear air turbulence (CAT) and was flown on a shake-down flight in 1972 and in a search for CAT in 1973. The system succeeded in measuring clear air returns up to an altitude of 6 kilometers, and, on one occassion, detected mountain-wave turbulence, which was verified by penetration with the aircraft (ref. 2). The Lidar was found to be operating considerably under its theoretical expectations and was extensively refurbished, incorporating a number of changes including an offset local oscillator to allow ground-based operation with stationary targets. A series of ground tests was undertaken in 1977 and 1978, and the Lidar was flown in another CAT flight series in early 1979. Data analysis from this test series is still underway, so this paper will provide only representative selections of the types of information being obtained.

The Lidar is currently being modified to perform flow-field mapping of the non-precipitating regions of severe storms. This primarily involves the incorporation of a scan system, central timing and control system, new signal processing electronics, and a new telescope. An extensive measurement program is being planned for the summer of 1981.

SYSTEM DESCRIPTION

A block diagram of the Lidar is shown in Figure 2. It is a CO_2, pulsed, coherent Lidar operating at 10.6μm. Its configuration is known as a MOPA, (master oscillator power amplifier). To obtain an understanding of how the system operates, it is perhaps best to follow through the block diagram. First, the master oscillator is a continuous wave (CW) laser providing approximately 8 watts of linearly polarized radiation at 10.6μm. A small portion of this output is picked off for use in frequency stabilization of the master laser and for use in an offset locking loop used to maintain the offset-local-oscillator laser at a 10 MHz frequency offset from the master laser. The main portion of the master-laser output is directed to an electro-optic CdTe modulator, where it is chopped into a pulse train of variable width and rate. The width may be selected at 2,4, or 8 μs and the rate may be varied from 1 to 200 pulses per second. The resultant pulse train passes through an indium-antiomonide isolator which prevents reflections from the secondary mirror of the telescope from entering the master laser cavity. The pulse train, after being expanded to a diameter of 15mm, is then directed into a 6-tube power-amplifier array which provides approximately 40 dB of gain. The pulse train next passes through a Brewster window, a quarter-wave plate (which converts the polarization from linear to circular) and into a collimated 30cm diameter telescope where the pulse train is expanded to approximately 24 cm ($1/e^2$) and directed into the atmosphere. These pulses are scattered by particulates on the order of from 1 to 10 μm in size which are naturally entrained in the atmosphere. Some of the scattered light returns along the same optical path as the incident beam, after having been Doppler shifted in frequency by an amount proportional to the radial component of the aerosol velocity, and reversed in its direction of circular polarization. Measurement of this Doppler Shift in frequency is the primary purpose of the Lidar. The backscattered beam is collected by the telescope, passed through the quarter-wave plate and reflected by the Brewster window to the HgCdTe detector, where it is mixed with the LO beam. The reflection from the Brewster plate is enhanced by the change in polarization at the target, which results in linear polarization of the scattered beam at 90° to the polarization of the transmitter.

SYSTEM CAPABILITY SUMMARY

The System's range capability is determined by characteristics of the atmosphere and of the system. At the present time, the system's minimum range is 3 kilometers, due to detector saturation caused by the backscattering of transmitted light from the secondary mirror. Except for highly reflective targets such as clouds or the ground, the usual maximum range at which signals are received is limited by beam propagation effects to less than 15 kilometers. In the recent flight tests useful signals were obtained with backscatter coefficients estimated at $2 \times 10^{-9} m^{-1}$ steradian^{-1} or less. Particle sampling measurements have been used to predict CO_2 backscatter coefficients, and these analyses indicate a wide spread in the atmospheric backscatter coefficients. A new measurement program is being planned to make quantitative backscatter measurements at different altitudes, locations, and times to more accurately determine the operational capability of the system.

The resolution of the system in space, velocity and time may be varied within some limitations. Typical operation of the system during the CAT flight tests used an 8 microsecond pulse, resulting in a velocity resolution of 0.5 m/sec and a range resolution of 1.2 kilometers. The actual range or velocity estimate for a target may be improved by approximately $\sqrt{N}$ by integrating N pulses and them employing adaptive thresholding and statistical analysis.

The pulse repetition frequency of the system is typically 140 pulses per second, and, in typical operation, 25 to 50 pulses are integrated to produce a single data sample. This results in 3 to 6 data samples per second. During previous tests each data sample has included complete spectral data over a 10 megahertz (50 m/sec) bandwidth for a single selected range gate. A new processor, presently being installed, will provide processed spectral parameters for each range gate over the same range of data rates. Thus, while complete spectral data will not be available, parameters from all range gates will become available at the specified update rate. This will result in considerably more efficient use of the available data.

The display capabilities of the system include the real-time analog displays of processor outputs, near-real-time displays of algorithm results from the on-line mini computer, and more detailed displays which may be obtained at the completion of a mission. The real-time analog displays include the RVI, IVI, and A-Scope. These displays are shown in Figure 3. The top display is the RVI, which displays range on the horizontal axis, velocity on the vertical axis, and amplitude with intensity modulation of the display. At short ranges, the display in the

figure shows the saturation effect mentioned previously. At longer range, it shows a velocity which decreases and then increases with increasing range, along with varying amplitudes and spectral widths, and a distant return from a cloud or solid object. While this three-dimensional display is useful for a qualitative evaluation of the system, and for locating interesting features, it is not amenable to quantitative analysis. For these purposes, two-dimensional displays are more useful, and two such displays may be obtained by looking at slices of the RVI display, as indicated by the lines in the figure. The IVI shows the spectrum of the return at a selected range. The logarithm of the intensity is plotted as a function of frequency (velocity). This represents a vertical slice at a selected range through the RVI display. The A-Scope provides the opposite type of displays, showing the variations in intensity as a function of range at a selected velocity. In the indicated display, the atmospheric return has contributions at the selected velocity at two different ranges. The range scale is selectable, but is generally set at 16 kilometers, full scale. The on-line mini computer provides a means for recording the Lidar processor data, ancillary data from other sources, time and run number, and provides selected parameter displays. For example velocity, spectral width, or amplitude could be plotted with respect to time, range, or other parameters. The mini computer provides a number of default displays, and additional displays can be selected by the operator. All data are recorded on magnetic tape for more detailed analysis with the mini computer or with an off-line large-scale computer.

AIRBORNE MEASUREMENTS

During the 1979 flight tests, many different measurements were made to verify the different operational capabilities of the system. Calibration measurements were made using reasonably uniform hard targets, such as the desert floor to determine the system sensitivity. Velocity comparisons were made to verify measurements of the correct Doppler frequency. Power spectral density measurements of the atmospheric velocity were made as well as actual measurements of clear air turbulence encounters. This section will describe one of each of these types of measurements.

Several approaches were made at various solid targets to establish the sensitivity of the system. The most consistent results were obtained from the desert sand at Edwards AFB. Knowing the reflectivity $\rho(\pi)$ of the solid target and the pulse length, $\Delta \ell$, it is easy to calculate the atmospheric backscatter coefficient which would produce the same signal;

$$\beta_1 (\pi) = \rho (\pi)/\Delta \ell. \tag{1}$$

532

The minimum detectable backscatter coefficient is in the same ratio to this as the minimum detectable signal is to the calibration signal;

$$\frac{\beta_{min}(\pi)}{\beta_1(\pi)} = \frac{SNR_{min}}{SNR_1} \qquad (2)$$

From this, the estimate of $\beta_{min}(\pi) = 2 \times 10^{-9} m^{-1} steradians^{-1}$ was obtained.

A comparison of the ground speed as measured by the Doppler Lidar to that measured by the aircraft Inertial Navigation System (INS) is shown in figure 4. These measurements were made during flight 28 on March 26, 1979. The aircraft plot was constructed by simply plotting the ground speed as measured by the aircraft INS. The Lidar plot was somewhat more complicated to construct, since the ground return had to be tracked in range as the dive progressed. This was accomplished by scanning in range, identifying the ground return in each scan by its amplitude characteristics, and calculating the mean of the signal spectrum through an automatic thresholding routine. The ground speed was then determined by multiplying the resultant velocity by the cosine of the pitch angle, taking into account the -1.5 degree offset for the pointing of the Lidar pod. The average difference in these ground speed measurements is 4.52 meters per second with a standard deviation of 0.6 meters per second. During the flight, comparison of airborne digital data acquisition system (ADDAS) with cockpit data indicated that the ADDAS-system velocity data were approximately 3 meters per second slow. The remaining 1.5 meters per second difference between the Lidar and the aircraft velocity measurements lies well within the error bounds of the aircraft measurement system.

A 13-minute segment of the mean wind-velocity component in the direction of the aircraft heading is shown in figure 5. This was measured 3 kilometers in front of the aircraft at an altitude of approximately 8.5 kilometers. Overall variations of approximately 8 m/s are indicated for the duration of the sample. This plot was produced by calculating the mean velocity of the spectrum, averaged over 50 pulses, at a rate of roughly 3 times a second. This time history has been corrected for ground-speed component in the measurement direction. This was obtained by multiplying the ground speed by the cosine of the drift angle (the angle between the aircraft heading and the actual direction of travel).

The power spectral density plot for this sample is shown at the bottom of figure 5. This plot was produced using a 2048 point FFT with Blackman windowing and the mean extracted. As can be seen from the plot, the -5/3 slope, predicted by Kolmogorov, is followed rather well out to a frequency of about .15 Hz

where it tends to level off to noise. At an airspeed of approx-
imately 235 m/s this corresponds to a spatial length of about
1.5 kilometers, which corresponds reasonably well to the pulse
length of about 1.2 km. It was anticipated that turbulence
length scales below this length would not be resolved by this
technique. However, turbulence length scales below this limit
do contribute to the spectral spread of the Lidar signal. Con-
sequently by combining this technique with spectral processing
of the Lidar signal, turbulence length scales from several
hundred kilometers (such as the case above) down to several
meters can be measured. The lower limit is determined by such
inherent effects as signal-to-noise ratio, processor bandwidth,
and spectral broadening caused by system characteristics.

An example of spectral broadening associated with clear
air turbulence is shown in figure 6. This figure shows, on a
single plot, the spectral broadening due to turbulence length
scales less than the pulse length and the accelerations actually
encountered by the aircraft. In this case, the broadening of
the spectrum occurs about 20 seconds before the turbulence
encounter. An automated analysis of selected turbulence encoun-
ters and additional analysis of power spectral densities at the
longer turbulence scales are in the process of being implemented.

FUTURE PROGRAMS

The Lidar is presently being modified to perform measure-
ments of the clear-air regions around severe storms. The
transmitter will be overhauled and a new off-axis telescope ob-
tained, which will eliminate the saturation effects at near
ranges (caused by reflections from the secondary mirror in the
present telescope). A scan system is being constructed which
will allow the scan pattern shown in figure 7. This type of
scanning will allow the measurement of the mean wind velocity
components in a region from two different view angles, thereby
allowing resolution of the horizontal vector wind velocity.

A new signal processing system is being installed which will
calculate the spectral power, mean frequency, and width for each
range gate for every integration period. This information will
be fed to a central timing and control system, which incorpor-
ates the location data from the scanner and the aircraft and
interfaces to an on-line PDP11-35 computer for processing.

The output of this measurement will be in the form of a
two-dimensional vector map of the velocities in the horizontal
plane at the altitude of the aircraft.

A flight test of this system is planned for June and July
of 1981. Successful results in this test will, in all probabil-
ity, lead to additional measurements being performed in 1982

and 1983.

Because of the importance of atmospheric-backscatter-co-efficient levels to system operations, a test program has been undertaken to develop and fly a compact, CW, Doppler Lidar. This program is aimed specifically at establishing the back-scatter-coefficient variation with altitude and location. A long-term program to attempt to establish the temporal as well as spatial variation over the next 3 years is being planned.

SUMMARY

An airborne Doppler Lidar has been described which has been used successfully to detect turbulence and to perform large-scale wind variation measurements. The airborne measurement program, which took place in January through March 1979, was conducted by personnel from the Raytheon Company and Marshall Space Flight Center. The real-time and post-processing software utilized in obtaining the selected data samples were provided by the M&S Computing Corporation. Post-processing software for data generated on the Univac 1108 computer was provided by Computer Science Corporation. The flight operations were performed by Ames Research Center and meteorological support was provided by Dryden Flight Research Center, the United States Air Force, Stanford Research Institute and Marshall Space Flight Center. Particulate studies were performed by Alabama A&M University.

REFERENCES

1. Development of CO_2 Laser Doppler Instrumentation for Detection of Clear Air Turbulence, Final Report 10 February 1972 - 27 December 1978, ER78-4392-1 NASA Contract NAS8-28424, C.E. Harris, A.V. Jelalian

2. Huffaker, R.M., "CO_2 Laser Doppler Systems for the Measurement of Atmospheric Winds and Turbulence," Atmospheric Technology, NCAR, Winter, 1974-75.
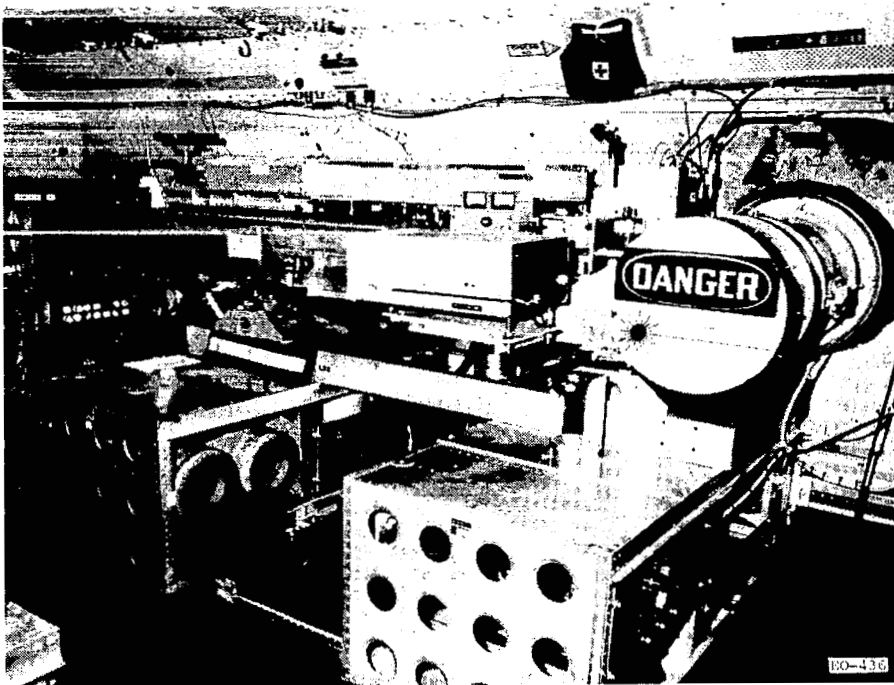
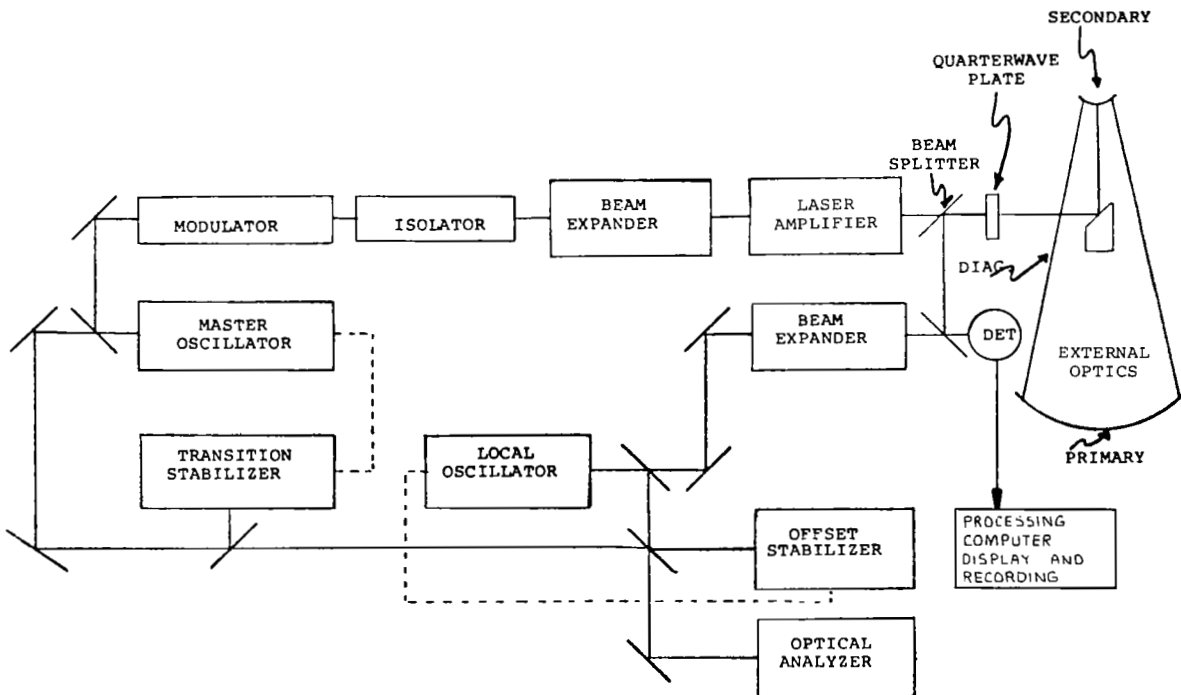Figure 1.- Pulsed CO_2 Doppler Lidar in aircraft.
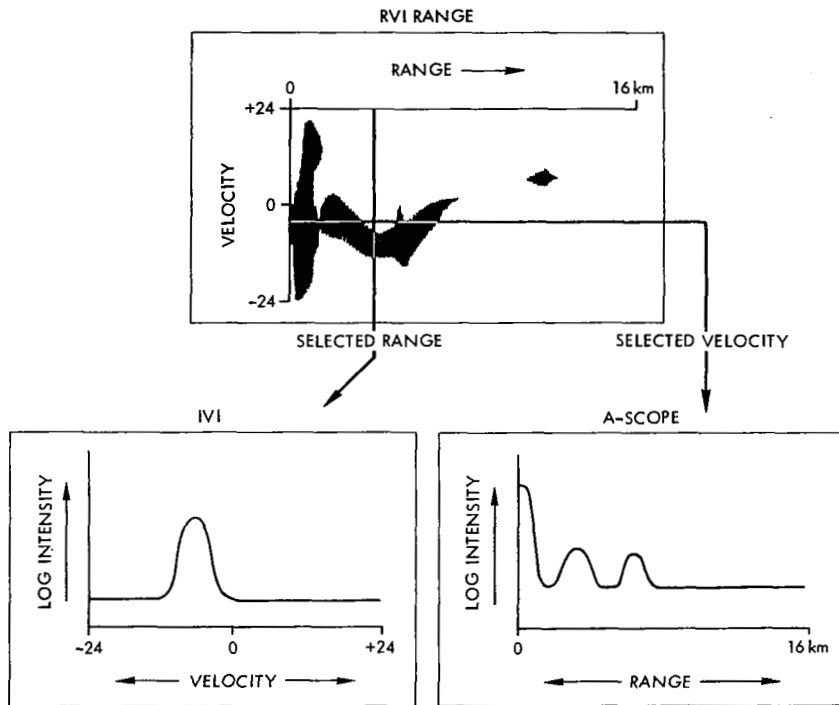

Figure 2.- Pulsed CO_2 Doppler Lidar block diagram.

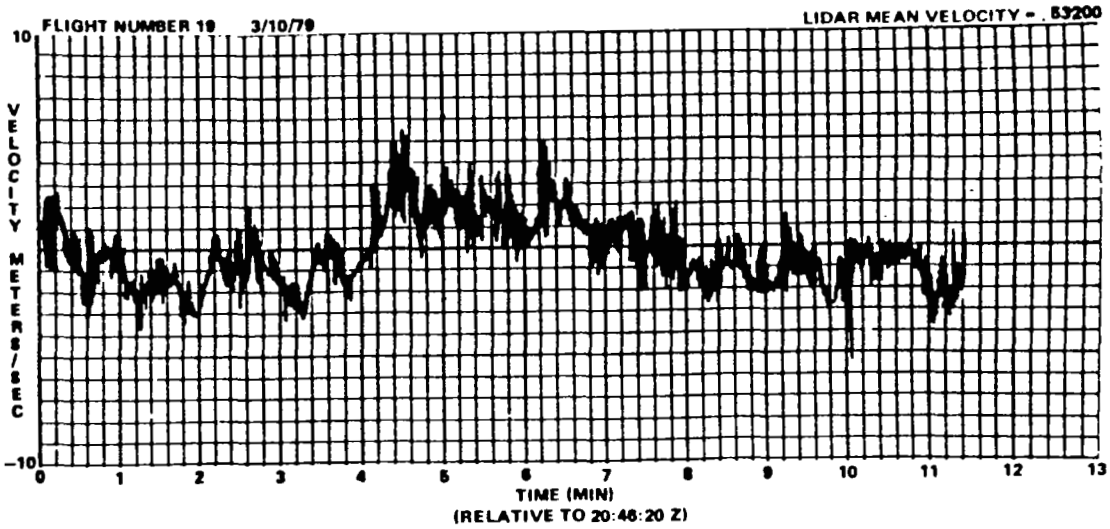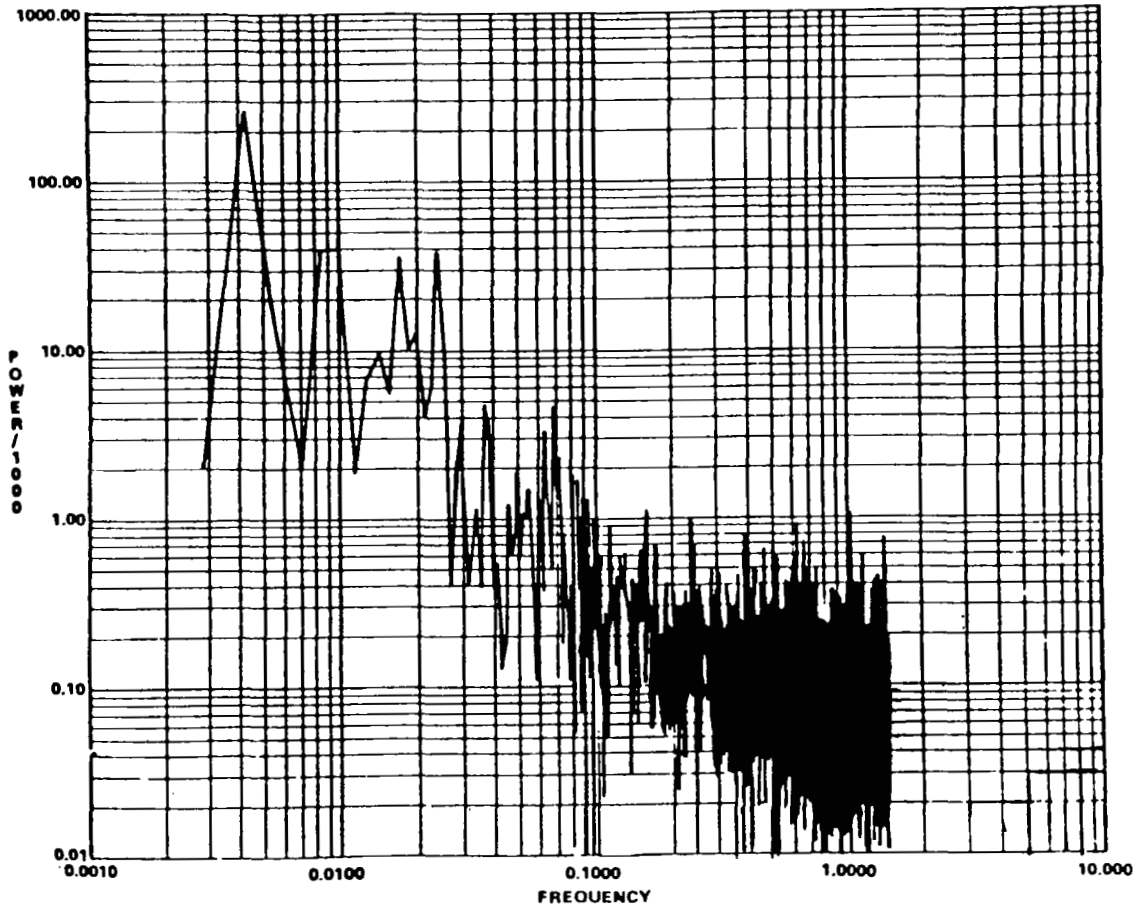Figure 3.- CAT detection real-time displays.
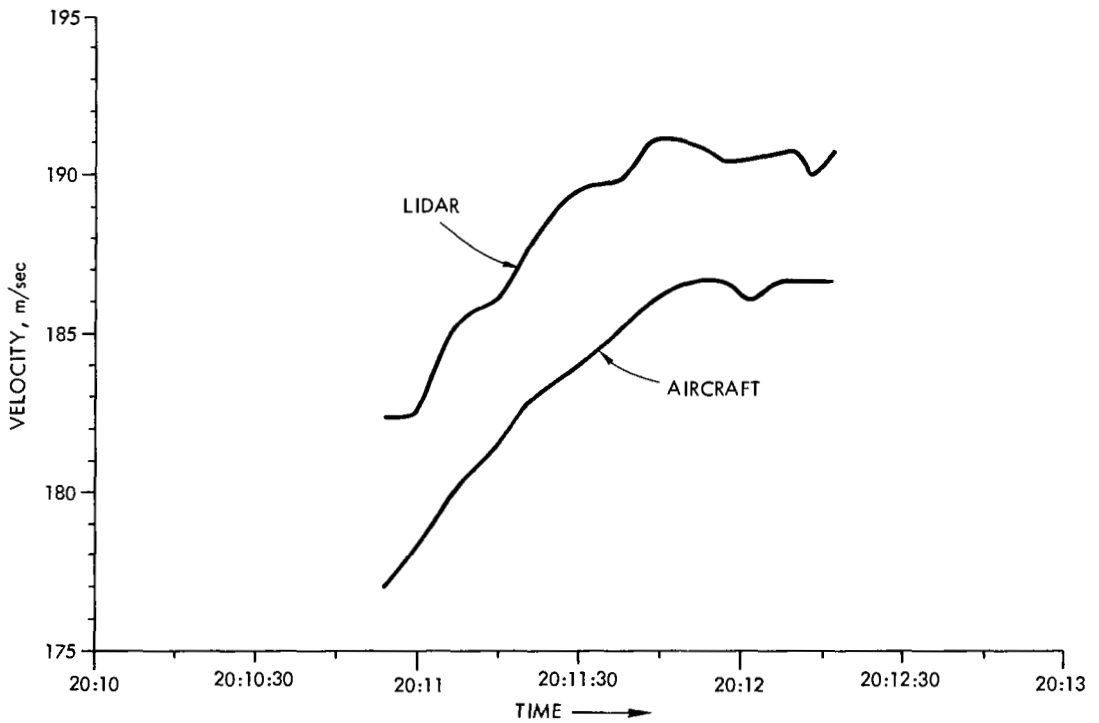
Figure 4.- Pulsed CO_2 Doppler Lidar velocity comparison using ground as a target.

A. VELOCITY TIME HISTORY

B. POWER SPECTRAL DENSITY

Figure 5.- Atmospheric-velocity measurements with a pulsed CO_2 Lidar.
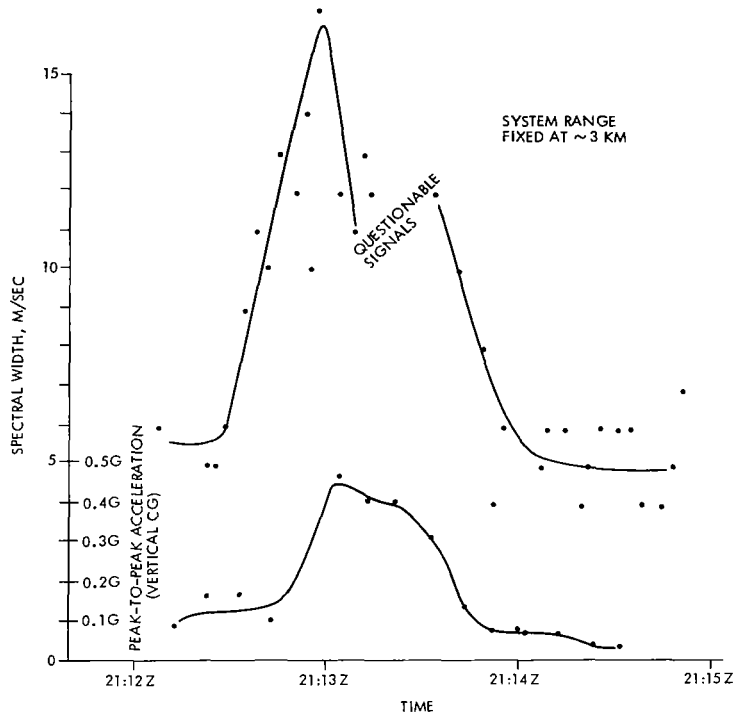
Figure 6.- Time history of a CAT encounter.

Figure 7.- Severe storm measurement concept.